

## Indication of Unusual Pentagonal Structures in Atomic-Size Cu Nanowires

J. C. González,<sup>1</sup> V. Rodrigues,<sup>1</sup> J. Bettini,<sup>1</sup> L. G. C. Rego,<sup>2</sup> A. R. Rocha,<sup>3</sup> P. Z. Coura,<sup>4</sup> S. O. Dantas,<sup>4</sup> F. Sato,<sup>5</sup>  
D. S. Galvão,<sup>5</sup> and D. Ugarte<sup>1,5,\*</sup>

<sup>1</sup>Laboratório Nacional de Luz Síncrotron, C.P. 6192, 13084-971 Campinas, SP, Brazil

<sup>2</sup>Departamento de Física, Universidade Federal de Santa Catarina, 88040-900 Florianópolis, SC, Brazil

<sup>3</sup>Department of Physics, Trinity College Dublin, Dublin 2, Ireland

<sup>4</sup>Departamento de Física, ICE, Universidade Federal de Juiz de Fora, 36036-330 Juiz de Fora, MG, Brazil

<sup>5</sup>Instituto de Física Gleb Wataghin, Universidade Estadual de Campinas, C.P. 6165, 13083-970 Campinas, SP, Brazil

(Received 18 May 2004; published 17 September 2004)

We present a study of the structural and quantum conductance properties of atomic-size copper nanowires generated by mechanical stretching. The atomistic evolution was derived from time-resolved electron microscopy observations and molecular dynamics simulations. We have analyzed the quantum transport behavior by means of conductance measurements and theoretical calculations. The results suggest the formation of an unusual and highly stable pentagonal Cu nanowire with a diameter of  $\sim 0.45$  nm and  $\sim 4.5$  conductance quanta.

DOI: 10.1103/PhysRevLett.93.126103

PACS numbers: 81.07.Lk, 68.65.-k, 73.50.-h, 73.63.Rt

Metal nanowires (NW's) exhibit quantum conductance properties even at room temperature [1]. This fact renders them a fundamental issue, because the development of nanoelectronic devices will require atomic-size contacts, or nanometric conductors for wiring. When a system attains nanometric size, the high surface/volume ratio induces unusual atomic structures that give rise to novel physical behaviors. Weird NW structures have been theoretically predicted [2], and recently helical or tubular gold NW's have been reported [3,4]; however, their quantum transport properties have not yet been measured.

NW's can be generated by putting in contact two metal surfaces, which are subsequently pulled apart. During the stretching, the conductance displays flat plateaus and abrupt jumps of approximately a conductance quantum  $G_0 = 2e^2/h$  ( $e$  is the electron charge,  $h$  is Planck's constant [1]). Recently, these studies have led to the discovery of suspended linear chains of atoms (LAC's) [5,6], whose conductance is equal to  $1G_0$  for monovalent metals such as Au [5–8] or Ag [9]. Surprisingly, although copper is a usual interconnect metal, Cu NW's have not yet been studied in detail [10].

The elongation of metal contacts is a rather simple experimental procedure. However, this experiment yields a large variety of quantum conductance curve profiles (QCC, conductance versus a parameter describing the elongation), because each curve corresponds to the structural evolution of a different NW. To overcome this difficulty, most studies analyze average behaviors: First, each QCC is plotted as a histogram of conductance occurrences. Subsequently, a global histogram (GH) is constructed by the linear addition of the histograms. The existence of GH peaks close to integer multiples of  $G_0$  has been considered the proof of quantized conductance in NW's [1].

In this work, we have experimentally and theoretically studied the structural and conductance behavior of Cu

NW's. Our study provides clear indication for the formation of pentagonal Cu NW's with a conductance of  $\sim 4.5G_0$ .

Experiments based on time-resolved high resolution transmission electron microscopy (HRTEM, JEM-3010 URP 300 kV, 0.17 nm point resolution) have been used to study the atomic arrangement. NW's were generated *in situ* using the procedure proposed in [11], where holes are opened at several points of a self-supported metal film by focusing the microscope electron beam ( $\sim 120$  A/cm<sup>2</sup>). When two holes are very close, nanometric bridges are formed between them, then the beam current is reduced to its conventional value (10–30 A/cm<sup>2</sup>) for image acquisition [12]. A polycrystalline Cu film ( $\sim 30$  nm thick) was sandwiched between two ( $\sim 3$  nm thick) amorphous carbon layers. The three-layer configuration allows the Cu film to be transferred into the HRTEM without oxide formation [13]. Inside the microscope, the carbon layers are removed by electron irradiation [12]. The NW elongation process was recorded using a high sensitivity TV camera (Gatan 622SC).

The electrical properties of Cu NW's were investigated, in a series of independent experiments, using a mechanically controllable break junction method operating in ultrahigh vacuum (pressure  $\leq 10^{-10}$  mbar) [7]. In this method, a Cu wire (diameter  $\sim 0.075$  mm, 99.999% pure) is broken *in situ*; NW's are generated by putting in contact and subsequently retracting these surfaces. A homemade voltage source and a current-voltage converter coupled to an eight-bit digital oscilloscope (Tektronic TDS540C) were used to record the conductance [7].

The analysis of many HRTEM observations of Cu NW's reveals that the wire structure adopts merely three configurations, where the elongation direction follows the [100], [110], and [111] crystal axes of the Cu face centered cubic (fcc) structure. Figure 1 shows some snapshots of the final elongation steps along these axes. The formation

of rodlike wires was observed for NW's along [100] and [110] directions [Figs. 1(a) and 1(c), respectively]. In contrast, NW's along [111] [henceforth noted as [111] NW's, Fig. 1(b) and 1(d)] exhibit a bipyramidal shape. All NW's evolve to generate short atomic chains before rupture [Figs. 1(b) and 1(d) and 1(f)].

Figure 2 shows the measured conductance behavior of Cu NW's. The GH shows major peaks at  $1$ ,  $2.4$ , and  $4.5G_0$ , the latter one being the strongest. Though the GH analysis represents a powerful tool, it is essential to also analyze individual QCC's, which provide a wealth of physical information [7–9,12]. In fact, the quality of this kind of experiments can only be evaluated from QCC's. For example, plateaus must be mostly horizontal, jumps must be vertical, and the final rupture must be abrupt without minor substeps ( $0.1$ – $0.2G_0$ ) close to zero conductance [as shown in Fig. 2 (inset)]. Deviations from the precedent requirements could indicate the existence of contamination during the NW conductance experiment. The Cu GH is quite different from other noble metals; Au GH is dominated by the  $1G_0$  peak with a minor contribution at  $1.8G_0$  [1,7,12], while Ag GH shows major peaks at  $1G_0$  and  $2.4G_0$  [9]. As the QCC profile is a signature of the NW structural evolution [1,7,8], the GH peaks pinpoint the most stable atomic structures [1,7,9,12]. In these terms, the Cu GH follows the Ag behavior for the  $1.0$  and  $2.4G_0$  regions, but the strong  $4.5G_0$  peak reveals a new highly stable structure for Cu NW's.

The three-dimensional atomic arrangement of the NW's can be inferred from HRTEM images by means of the geometrical Wulff construction [14]. This method yields the crystal shape by predicting the relative size of the lower-energy facets of the crystal. Recently, it has been successfully applied to describe the morphology of

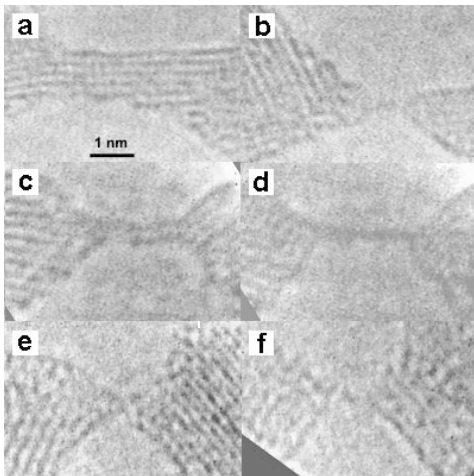


FIG. 1. HRTEM atomic resolved images showing the formation of Cu NW's along different crystallographic directions: (a),(b) [100]; (c),(d) [110]; (e),(f) [111]. Note that suspended atom chains are formed just before rupture for all three directions (b),(d),(f).

Au and Ag NW's [7–9,12], taking as basis the predicted morphology of the corresponding nanoparticles (see top of Fig. 3, marked A and B for Au and Ag, respectively). As for Cu, HRTEM images have recently shown that the morphology of  $\sim 5$  nm diameter Cu nanoparticles is a truncated cuboctahedron with dominant [100] facets [15,16]; then, qualitatively, a Cu nanoparticle must have a morphology closer to particle marked C in Fig. 3. Considering this nanoparticle along the [100] direction, we can infer that a [100] rodlike NW would show a square cross section bounded by four (100) planes [Fig. 3(a)]. Likewise, a [110] rodlike NW would show a hexagonal cross section bounded by two large (100) facets and four smaller (111) facets [Fig. 3(b)]. On the other hand, [111] NW's should present a bipyramidal shape with each pyramid bounded by three large (100) facets and, less probably, three small (111) facets (see particle marked as C in Fig. 3). In Fig. 3, the notation  $n/m$ , over each proposed NW structure, means that the NW would be generated by the alternate stacking of atomic planes with  $n$  and  $m$  atoms along the elongation direction (atomic planes are marked with different tones in the figure). This simple model shows an excellent agreement with the NW morphologies presented in Fig. 1.

In order to correlate the deduced wire structures (Fig. 3) with the electrical properties, we have calculated the conductance using an approach based on the extended Hückel theory [8,17]. This model has already been successfully used to calculate the conductance of Au and Ag NW's [8,9]. The calculations have taken into account the  $s$ ,  $p$ , and  $d$  orbitals of Cu atoms in the NW, as well as overlap and energy matrix elements extending beyond the first-neighbor atoms. Table I summarizes predictions for different NW's derived from a perfect fcc structure.

As expected, LAC's display conductance close to  $1G_0$  for all apex crystal orientations ([100], [110], and [111]).

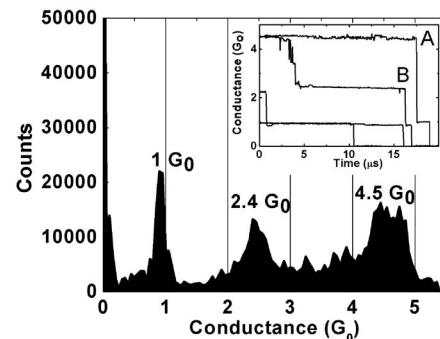


FIG. 2. Ultrahigh vacuum-mechanically controllable break junction conductance measurements of Cu NW's at room temperature. Global histogram exhibiting the statistical conductance behavior of a sequence. (Inset) Typical electrical transport curves showing conductance plateaus of NW generations. Note that the major GH peaks are located at  $\sim 1$ ,  $2.4$ , and  $4.5G_0$ .

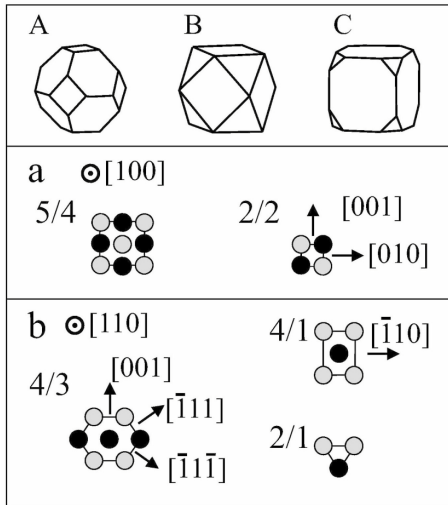


FIG. 3. (A)–(C) Geometrical shapes of cuboctahedral nanoparticles increasing the relevance of [100] facets (or lowering the facet surface energy) in relation to [111] facets. Scheme of the possible atomic arrangements for Cu NW's: (a) and (b) cross section of NW's formed along [100] and [110] axes, respectively, (see text for explanations).

In analogy to previous studies on Ag wires [9], the  $2.4G_0$  GH peak can be associated with the [110] rodlike Cu wire with a 2/1 structure. Finally, the  $4.5G_0$  GH peak can only be accounted for the 5/4 [100] rods. Several proposed structures would display conductances (e.g., 1.8 or  $3.8G_0$ ) that do not appear as statistically meaningful in the Cu GH. These atomic arrangements must be considered as low stability ones [8,9] and will be excluded in further analysis.

The precedent correlation between GH peaks and proposed structures represents a preliminary picture, and it is essential to analyze individual QCC profiles, which provide precise information on individual NW structural evolution [1,8]. For example, two kinds of QCC's [marked A and B in Fig. 2 (inset)] have plateaus at  $\sim 4.5G_0$ . Curve A evolves from 4.5 to  $1G_0$ , which can be explained by a 5/4 [100] rod converting into a LAC structure. Curve B shows three plateaus at  $\sim 4.5$ ,  $\sim 2.4$ , and  $\sim 1G_0$ . In this case, the interpretation is not straightforward, because a jump from 4.5 to  $2.4G_0$  would imply a change of NW elongation direction (i.e., 5/4 [100] into a 2/1 [110] NW).

To refine the structural analysis, we can use the criterion proposed by Rodrigues *et al.* [7] to predict Au QCC occurrence rates. This approach takes into account the multiplicity of the crystal axis associated to the elongation direction (three for [100], four for [111], and six for [110]; a total of 13 possibilities). As both Cu and Au display an fcc structure, their analysis [7] can be directly applied to our Cu wire results. In this sense, [100] wires [A-like curves, Fig. 2 (inset)] would represent a 3/13 fraction (23%) of the total number of measured QCC's, while [110] NW's [B-like curves, Fig. 2 (inset)] would

represent a 6/13 fraction (46%). A visual counting of QCC profiles (450 curves in total) yields that A-like curves represent 28%, while B-like curves represent 46% of the analyzed curves. This confirms the assignment of A-like and B-like curves as the evolution of [100] and [110] NW's, respectively, but raises an intriguing question on the origin of a  $4.5G_0$  plateau for [110] rodlike NW's. In fact, the  $4.5G_0$  GH peak is the major difference between the Cu and Ag or Au NW's [1,7,9], and it can not be explained by structures derived from a geometrically perfect fcc crystal.

For noble metal nanoparticles, it is well known that the surface energy minimization may induce the formation of multiple-twinned particles (e.g., decahedra, icosahedra) [14] containing twins and five-fold axes. In fact, icosahedral or decahedral structures have already been reported as the preferred ones for small Cu particles [15,16,18]. Furthermore, Cu NW's with pentagonal cross section and axis along [110] direction have already been chemically synthesized [16]. Sen *et al.* [19] have used first-principles calculations to study two pentagonal Cu NW's along the [110] direction (decahedral or icosahedral motifs) and concluded that these wires should be stable and metallic. The smallest pentagonal NW's are formed by the alternate stacking of a pentagonal atomic plane containing five atoms and a second plane including one atom on the central axis (5/1d); icosahedral NW's (5/1i) are built in similar way, but the pentagons are rotated  $\pi/10$  with respect to each other [19].

We have estimated the conductance of the relaxed pentagonal atomic arrangements [19] and both 5/1d and 5/1i NW's exhibit conductance  $\sim 4.5G_0$ . To couple the wires to the electron reservoirs, we have used decahedral apexes with ideal geometrical structure. Since Cu atoms in neighboring pentagonal planes are approximately at the nearest neighbor distance (0.256 nm), the presence of a central Cu atom between pentagonal planes is not enough to render the nanowire conductance close to  $1G_0$ . We have also calculated 2/1 [110] NW's derived by the thinning of a pentagonal wire considering atomic arrangements that were either unrelaxed or relaxed fol-

TABLE I. Calculated quantum conductance for NW's derived from a geometrically perfect fcc structure (see text for explanations).

Elongation Axis	Structure	Conductance [ $G_0$ ]
[100]	5/4	4.5
	2/2	1.8
[111]	10/6/8	6.2
[110]	4/3	5.5
	4/1	3.8
	2/1	2.4
	1/1	1.8

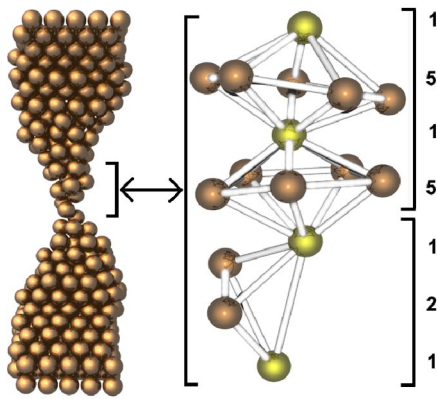


FIG. 4 (color online). Atomic arrangement during the last stages of stretching of a Cu NW along a [110] direction obtained by means of molecular dynamics simulations. At the right side, the numbers indicate the quantity of atoms located in different atomic planes along the elongation axis. Note that the formation of a pentagonal structure is clearly indicated by the 1/5/1/5/1 sequence. Also the evolution of this structure into a 2/1 NW is revealed by the snapshot.

lowing the approach proposed by Sen *et al.* [19]. All these 2/1 [110] wires display a conductance very close to  $2.4G_0$ . These results indicate that the [110] Cu NW conductance evolution ( $4.5$ ,  $2.4$ ,  $1G_0$ ) can be fully explained by considering pentagonal 5/1 Cu NW's along the [110] axis.

Unfortunately, we have not been able to reveal the formation of pentagonal NW's by HRTEM, because the lower atomic number of Cu and its small lattice parameter have rendered quite challenging the atomic resolution observation of Cu NW's. To get more insight into the structural evolution, we have used tight-binding molecular dynamics simulations using second-moment approximation [20–22]. Figure 4 shows a snapshot of a Cu NW being elongated along the [110] axis [23]. The inset shows a closer view of the atomic arrangement, where the formation of pentagonal wires with a 5/1 structure can be easily identified. Also, we must note that the narrowest NW sector shows an 2/1-type atomic arrangement being formed from a 5/1-type structure. These structural patterns have been frequently observed in [110] Cu NW's but not for NW's along [100] and [111] directions. These results show an excellent agreement with our conductance and structural analysis.

In summary, we have obtained experimental and theoretical indications that Cu nanowires generated by mechanical stretching should show structural relaxation forming pentagonal [110] Cu NW's with a quantum con-

ductance of  $\sim 4.5G_0$ . Finally, considering that Ag [110] NW structural behavior is very similar to Cu and also that Ag GH shows a minor peak at  $4.5G_0$  [9], it is possible that 5/1 pentagonal Ag NW's could also be generated by stretching.

This work was supported by LNLS, CNPq, FAPESP, IMMP/MCT, and CAPES/PRODOC.

\*Electronic address: [ugarte@lnls.br](mailto:ugarte@lnls.br)

- [1] N. Agrait, A. L. Yeyati, and J. M. van Ruitenbeek, *Phys. Rep.* **377**, 81 (2003).
- [2] O. Gulseren, F. Ercolessi, and E. Tosatti, *Phys. Rev. Lett.* **80**, 3775 (1998).
- [3] Y. Kondo and K. Takayanagi, *Science* **289**, 606 (2000).
- [4] Y. Oshima, A. Onga, and K. Takayanagi, *Phys. Rev. Lett.* **91**, 205503 (2003).
- [5] H. Ohnishi, Y. Kondo, and K. Takayanagi, *Nature (London)* **395**, 780 (1998).
- [6] A. I. Yanson *et al.*, *Nature (London)* **395**, 783 (1998).
- [7] V. Rodrigues, T. Fuhrer, and D. Ugarte, *Phys. Rev. Lett.* **85**, 4124 (2000).
- [8] L. G. C. Rego, A. R. Rocha, V. Rodrigues, and D. Ugarte, *Phys. Rev. B* **67**, 045412 (2003).
- [9] V. Rodrigues *et al.*, *Phys. Rev. B* **65**, 153402 (2002).
- [10] J. M. Krans *et al.*, *Nature (London)* **375**, 767 (1995).
- [11] Y. Kondo and K. Takayanagi, *Phys. Rev. Lett.* **79**, 3455 (1997).
- [12] V. Rodrigues and D. Ugarte, in *Nanowires and Nanobelts*, edited by Z. L. Wang (Kluwer, Dordrecht, 2003), Vol. 1, p. 177.
- [13] V. Rodrigues, J. Bettini, P. C. Silva, and D. Ugarte, *Phys. Rev. Lett.* **91**, 096801 (2003).
- [14] L. D. Marks, *Rep. Prog. Phys.* **57**, 603 (1994).
- [15] J. Urban, *Cryst. Res. Technol.* **33**, 1009 (1998).
- [16] I. Lisiecki *et al.*, *Phys. Rev. B* **61**, 4968 (2000).
- [17] E. G. Emberly and G. Kirczenow, *Phys. Rev. B* **58**, 10911 (1998); **60**, 6028 (1999).
- [18] D. Reinhard *et al.*, *Phys. Rev. Lett.* **79**, 1459 (1997).
- [19] P. Sen *et al.*, *Phys. Rev. B* **65**, 235433 (2002).
- [20] F. Cleri and V. Rosato, *Phys. Rev. B* **48**, 22 (1993).
- [21] D. Tománek, A. A. Aligia, and C. A. Balseiro, *Phys. Rev. B* **32**, 5051 (1985).
- [22] P. Z. Coura *et al.*, *Nano Lett.* **4**, 1187 (2004).
- [23] See EPAPS Document No. E-PRLTAO-93-010436 for Figure 4 snapshot of a Cu nanowire being elongated along the [110] axis. A direct link to this document may be found in the online article's HTML reference section. The document may also be reached via the EPAPS homepage (<http://www.aip.org/pubservs/epaps.html>) or from <ftp.aip.org> in the directory `/epaps/`. See the EPAPS homepage for more information.